Transport of Central American Fire Emissions to the U.S. Gulf Coast: Climatological pathways and impacts on ozone and $PM_{2.5}$

Sing-Chun Wang[1,2], Yuxuan Wang[1,2], Mark Estes[3], Ruixue Lei[1,2], Robert Talbot[1,2], Liye Zhu[4], and Pei Hou[5,6]

[1]Department of Earth and Atmospheric Science, University of Houston, Houston, Texas, USA

[2]Institute for Climate and Atmospheric Science, University of Houston, Houston, Texas, USA

[3]Texas Commission on Environmental Quality, Austin, Texas, USA

[4]Department of Atmospheric and Oceanic Sciences, University of California, Los Angeles, California, USA

[5]Atmospheric Sciences Program, Michigan Technological University, Houghton, Michigan, USA

[6]Department of Geological and Mining Engineering and Sciences, Michigan Technological University, Houghton, Michigan, USA

Corresponding author: Yuxuan Wang (ywang246@central.uh.edu)

Key Points:

- Southerly low-level jets and warm conveyor belts are the main mechanisms transporting Central American fire emissions to the U.S.
- Large transport events were identified, accounting for ~9% of the study period.
- These large events increased daily MDA8 ozone and $PM_{2.5}$ in Gulf Coast cities by 3-12 ppbv and 2-5 $\mu g/m^3$, respectively.

This article has been accepted for publication and undergone full peer review but has not been through the copyediting, typesetting, pagination and proofreading process which may lead to differences between this version and the Version of Record. Please cite this article as doi: 10.1029/2018JD028684

Abstract

Fire emissions from Mexico and Central America are transported regularly to the U.S. Gulf Coast every spring under prevailing circulation patterns and affect U.S. air quality. Here we use a GEOS-Chem passive tracer simulation to develop the climatology of transport pathways of fire emissions over a long-term time period of April and May, 2002-2015 and estimate their adverse air quality effects for urban areas along the Gulf Coast. A conceptual model is presented to describe the transport mechanisms which involve southerly low-level jets (SLLJs) in the lower troposphere and warm conveyor belt (WCB) in the middle troposphere. The WCBs and the SLLJs explain 31% and 69% of the inter-annual variability of the mid-altitude (1.5-6 km) and low-altitude events (0-1.5 km), respectively. Considering both transport and fire emissions, approximately 9% of the study period (59-88 days of 854 days) were identified as large pollution events during which Central American fire emissions adversely impacted surface air quality at several major urban centers along the Gulf Coast, including Houston and Corpus Christi in TX, New Orleans in LA, Mobile in AL, and Pensacola in FL. Compared to clean maritime flow from the Gulf of Mexico, these events were estimated to result in average enhancements of maximum daily average 8-hr (MDA8) ozone and daily $PM_{2.5}$ (fine particulate matter < 2.5 μm in diameter) in the Gulf Coast cities of 3-12 ppbv and 2-5 $\mu g/m^3$, respectively. Only one ozone exceedance day (79 ppbv, on May 18, 2003) was found among the fire-impact days for the Houston region.

1. Introduction

Biomass burning is one of the primary sources of trace gases and aerosols in the global atmosphere (Andreae et al., 2001; Crutzen et al., 1990). Biomass burning emissions of nitrogen oxides (NOx) and volatile organic compounds (VOCs) can lead to elevation of tropospheric ozone (O_3) (Andreae & Merlet, 2001; Jaffe et al., 2004; Lu et al., 2016). Primary and secondary aerosols from biomass burning can influence air quality, cloud processes, and climate (Koren et al., 2004; Reid et al., 2005). Emissions from large fires can be injected above the boundary layer and efficiently transported far downwind and impact distant air quality.

As the anthropogenic emissions in the U.S. continue to decrease, the influence of fire emissions on U.S. air quality has become more important. For example, biomass burning in Central America has been shown to affect the U.S. air quality regularly in spring (Mendoza et al., 2005; Rogers et al., 2001; Yokelson et al., 2009). Satellite and surface observations have documented several cases of long-range transport of aerosol particles transported from Central American fires to the southern U.S. and the Gulf Coast (Leung et al., 2007; Saide et al., 2015; Saide et al., 2016; Wang et al., 2009). Most past studies focused on $PM_{2.5}$ pollution episodes caused by Central American fires. For example, Park et al. (2003) found that fires in Mexico and Canada contributed to 40-70% of the annual mean background concentrations of elemental carbon (EC) and 20-30% of organic carbon (OC) in the U.S. in year 1998. Wang et al. (2006) used in situ and space-based observations and a regional model to track and simulate smoke transport from Central America during April 20-May 21, 2003 and found that the smoke episode increased $PM_{2.5}$ by about 9 $\mu g/m^3$ at several surface monitors in Texas and Louisiana. Saide et al. (2016) identified 8 episodes of smoke transport from Central America to the U.S. during 2003-2014 based on satellite observations and simulated the effects of those episodes on tornado outbreaks in the U.S. Despite those well-studied episodes, the transport mechanism and climatological impact of these fires on ozone and $PM_{2.5}$ in the U.S. have not been fully investigated.

The Central American fire season peaks in spring (Apr-May) because of agricultural activities and dry weather (Peppler et al., 2000; Rogers & Bowman, 2001; Yokelson et al., 2009). In springtime, large circulation patterns over the Gulf of Mexico and North America are conducive for transporting pollutants from Central America to the U.S. These patterns include progressive mid-latitude synoptic systems and the persistent Bermuda High. The Bermuda High is a subtropical semi-permanent high-pressure center in the North Atlantic Ocean (Davis et al., 1997). Penetration of the Bermuda High into the Gulf of Mexico enhances low-level circulation with southeasterly to southwesterly winds from the Yucatan Peninsula to the Gulf Coast (Sáenz et al., 2015; Wang et al., 2016). These large-scale circulation patterns place the U.S. Gulf Coast directly downwind of Mexico and Central America, and thus subject to transport of pollutants originating there. After arriving over the Gulf Coast, the fire plumes can be further transported to the southern Great Plains or the southeastern U.S. (Logan et al., 2018; Peppler et al., 2000; Tanner et al., 2001). Wang et al. (2009) discussed other meteorological features facilitating the transport. For example, the presence of a low-pressure trough over the central U.S. enhances the southwesterly flow around the Bermuda High that can transport fire plumes continually to the Gulf Coast and southern Great Plains. The warm conveyor belt (WCB) associated with the trough can lift the smoke particles and transport them to far downwind. Eventually, the convective processes associated with the WCB or dry lines can lead to precipitation, which results in wet deposition and terminates smoke transport (Wang et al., 2009). While the above-mentioned circulation patterns in springtime are a well-known meteorological phenomenon, the role they play in the transport of Central American fire emissions in the long-term view is not fully appreciated.

The goals of this study are to develop the climatology of transport pathways of Central American fire emissions to the U.S. Gulf Coast and to quantify the contribution of those pollutants on surface ozone and $PM_{2.5}$ along the Gulf Coast. Although anthropogenic emissions in Central America can also affect the U.S. air quality, the scope of this study is focused on fire emissions from Central America. The study period is springtime (April and May) 2002-2015, the peak fire season in Central America. One major metropolitan area along the Gulf Coast is the Houston-Galveston-Brazoria (HGB) metropolitan area, which has a population of 5.3 million and has one of the most extensive air quality monitoring networks in the U.S. Thus, this impact analysis has an emphasis on the HGB area. We first use a passive tracer simulation of a chemical transport model to identify transport events of Central American fire emissions reaching the HGB area during the study period. We then examine the patterns of these transport events over the past fourteen years and investigate the transport mechanisms. Finally, we quantify the impact of Central American fires on surface ozone and $PM_{2.5}$ over the HGB area and the Gulf Coast, focusing on the strong transport events coincident with large fire emissions.

2. Data and Methods

2.1 Ozone and $PM_{2.5}$ observations

Figure S1 shows the ozone and $PM_{2.5}$ sites over the Gulf Coast cities used in the study. Ozone is measured either by chemiluminescence method or ultra violet method (Kleindienst et al., 1993; Regener, 1964). The ozone mixing ratio at all the sites used in this study have been qualified with the federal reference method (FRM) or federal equivalent method (FEM), which ensures the quality of the measurements and allows inter-comparison across sites (Hall et al., 2012). Observational data of the maximum daily average 8-hr (MDA8) ozone over the HGB area during the study period were obtained from the Texas Commission on Environmental Quality (TCEQ). For this study, the HGB region is defined by longitude from 94.5 to 96.0°W and by latitude from 28.5 to 30.5°N (black box in Figure 1). The continuous ambient monitoring stations (CAMS) sites that measured surface ozone in the HGB numbered 20 in 2002 and increased slowly to 46 in 2015. We obtained the daily HGB-mean MDA8 ozone mixing ratios by averaging across all of the available sites during the study period.

The ozone enhancement due to Central American fires would be considered a component of background ozone in the HGB area. The term "background ozone" has been defined in several ways to describe the amount of ozone imported into a given region (Fiore et al., 2002). For example, the policy-related background (PRB) ozone is defined by the U.S. Environmental Protection Agency (EPA) and is derived from model calculation with all anthropogenic emissions in North America removed (McDonald-Buller et al., 2011; Zhang et al., 2011). A related term is baseline ozone, which refers to the measured ozone level at sites with a negligible influence from local emissions, and this term is typically used to denote the ozone mixing ratios from the Pacific Ocean into the U.S. west coast (Parrish et al., 2009). Here we used the estimation of regional background ozone from the TCEQ, which is defined as the ozone that would be present in the area if no ozone were contributed by ozone precursors emitted locally on that day or prior days. It is estimated as the lowest MDA8 ozone value observed at the selected background sites over the HGB area (Berlin et al., 2013). For simplicity, the regional background ozone is referred to as background ozone hereafter.

Surface MDA8 ozone observations at other Gulf Coast cities, including Corpus Christi (2 sites), New Orleans (10 sites), Mobile (2 sites), and Pensacola (5 sites), were obtained from the EPA Air Data website (https://www.epa.gov/outdoor-air-quality-

data/download-daily-data). Numbers in brackets indicate number of ozone sites averaged for each city. For each of these cities, we averaged MDA8 ozone observations over all the available ozone sites on a daily basis. Corpus Christi is delineated by longitude from 96.87 to 98.87°W and by latitude from 27.5 to 28°N (blue box in Figure 1). The eastern Gulf Coast region is defined as a region between 87 to 97.5°W, and 27.5 to 31°N (red box in Figure 1).

Daily $PM_{2.5}$ observations at the Gulf Coast cities were obtained from the EPA AirData website. For a monitoring site which has more than one $PM_{2.5}$ sampling monitors, only the data measured by the primary monitor is used (Parameter of Occurrence Code=1). For each of these cities, we averaged $PM_{2.5}$ observations over all the available $PM_{2.5}$ sites on a daily basis. The daily $PM_{2.5}$ concentration was measured by different sampling methods including gravimetric method and beta attenuation method. These methods are classified as FRM or FEM, ensuring data quality and allowing for intercomparison of $PM_{2.5}$ observations. The overall data coverage at each selected city is over 80% during the study period, except for Mobile, which only has $PM_{2.5}$ observations every three days of all available sites, leading to limited availability of daily observations for Mobile (37% coverage during the study period).

2.2 Meteorological data

The meteorological data were obtained from European Centre Medium-Range Weather Forecasts (ECMWF) ERA-Interim reanalysis with a spatial resolution of 0.5°× 0.5°. We used the zonal (U) and meridional (V) components of wind at 10 m, the 2m temperature, relative humidity, and total precipitation to examine weather conditions over the HGB region. To present circulation patterns that are consistent with those used in the chemical transport model (Section 2.4), we used the meteorological data of U, V, geopotential height, and vertical pressure velocity from the Modern-Era Retrospective analysis for Research and Applications, version 2 (MERRA-2) with a spatial resolution of 0.5° x 0.625° at 850 hPa and 700 hPa.

Because clouds affect ozone photochemistry, we also examined the cloud field. We used daily cloud fraction observations retrieved from the MODerate-resolution Imaging Spectroradiometer (MODIS) Terra (MOD08_L3) with a spatial resolution of 1°x1°. MODIS Terra passes over the equator at approximately 10:30 LT and provides a large spatial coverage of cloud and aerosol measurements with a swath width of 2330 km. The cloud fractions were originally calculated in a 5 km x 5 km pixel using MODIS cloud masks (MOD35/MYD35) which have a 1 km resolution (Platnick et al., 2014). The products provide both daytime and nighttime observations. In this study, we only used daytime observations because they are directly related to the photochemical process in ozone formation.

To identify cyclone occurrences during the study period, we used the cyclone data from the National Snow & Ice Data Center (NSIDC) (https://nsidc.org/data/docs/daac/nsidc0423_cyclone/). The dataset contains the center location and pressure of the cyclones. Besides cyclone center information from the NSIDC database, synoptic patterns from the National Centers for Environmental Prediction (NCEP) weather maps were also used to identify the airstreams and fronts associated with the cyclones.

2.3 Satellite observation

Carbon monoxide (CO) and primary aerosols are emitted directly from biomass burning, and thus they are commonly considered as good indicators of fire plume transport. We used satellite observations of CO and aerosol optical depth (AOD) to illustrate the transport patterns of fire plumes and to verify whether fire plumes actually existed during the transport events identified by the model. We used CO observations from the Measurements of Pollution in the Troposphere (MOPITT) (Deeter et al., 2017; MOPITT Science Team,

2013; Worden et al., 2010) and AOD observations from MODIS (Remer et al., 2005). MOPITT is a sun-synchronous satellite and crosses the equator at 10:30 LT. The spatial resolution of MOPITT is 22 km with a swath 640 km wide scanning across the satellite track. MOPITT measures tropospheric CO in two channels: thermal-infrared (TIR) band (4.7μm) and near-infrared (NIR) band (2.3μm). The NIR measures the attenuation of reflection of solar radiation from the surface, while the TIR senses thermally-emitted radiation of CO from the surface and atmosphere. Thus, the NIR measurement focuses on the CO total column while the TIR radiances are sensitive to CO in the middle and upper troposphere. Additionally, the NIR can provide more sensitivity to lower tropospheric CO over land because of higher surface reflectance over land, thus providing supplemental information of CO mixing ratio in the lower troposphere (Deeter et al., 2007, 2009). In this study, the MOPITT Level 3 Version 7(V7) joint thermal and near infrared (TIR-NIR) daily mean gridded (1°x1° spatial resolution) CO products were used, which exploits both the NIR and TIR channels. The TIR-NIR product has higher sensitivity to CO in the troposphere compared to the previous TIR-only product (Worden et al., 2010). Only daytime MOPITT observations were used because Central American fires mostly occur in the daytime and there is little sensitivity near the surface for the NIR channel during nighttime. The MODIS aerosol products provide the aerosol optical depth (AOD) globally. We used retrievals of MODIS Level 2 Collection 6 AOD at 550 nm from the Terra satellite with a spatial resolution of 10 km × 10 km.

The Cloud-Aerosol Lidar and Infrared Satellite Observations (CALIPSO) satellite combines an active lidar instrument with passive infrared and visible imagers to provide the vertical structures of cloud and aerosol within a small footprint of 100 m (Winker et al., 2010). The CALIPSO crosses the equator at approximately 13:30 LT. The products of CALIPSO have been widely used to identify transport of dust and fire plumes in many studies (Dirksen et al., 2009; Huang et al., 2008; Liu et al., 2008; Miller et al., 2011). In this study, we used the vertical feature mask and aerosol subtype data from the CALIPSO data browse images to present transport of fire plumes for a case study.

2.4 GEOS-Chem model

Since current satellites can provide at most one or two measurements per day, we utilized a chemical-transport model (CTM), GEOS-Chem, to simulate the spatial and temporal variability of the transport of Central American fire emissions over the past 14 years. The GEOS-Chem model is a global 3-D CTM driven by the assimilated meteorological data from the NASA Goddard Earth Observation of the NASA Global Modeling and Assimilation Office (GMAO) (Bey et al., 2001). The GEOS-Chem model has been used in a number of studies on long-range transport of air pollutions (Jaffe et al., 2004; Liang et al., 2004; Sinha et al., 2004). We used GEOS-Chem with passive tracer simulation (see below) driven by MERRA-2 reanalysis data which has a native resolution of 0.5° × 0.625°. We conducted the nested-grid GEOS-Chem simulation (v11-01) with this native resolution over North America (130-60°W, 9.75-60°N) for the whole study period (April and May, 2002-2015), using lateral boundary conditions updated every 3 hours from a global GEOS-Chem simulation with a horizontal resolution of 2° × 2.5°.

2.4 Experimental Design

The focus of this study is on climatology and inter-annual variability of transport pathways of Central American fire emissions, which requires a long-term CTM simulation. A long-term (10+ years) CTM simulation with the full chemistry mechanism is computationally expensive and may not be necessary for the purpose of transport climatology. Therefore, in this study, we adopted the passive tracer simulation in GEOS-Chem to model the transport of

Central American fire emissions over the 14-year study period (April and May of each year). Since the fire emissions are expected to mix with clean maritime air masses from the Gulf of Mexico during transport, we designed two synthetic passive tracers in the model – the Gulf tracer and the Central American fire tracer (fire tracer hereafter) – to separately track the two types of air masses of similar transport route but different source signatures from the receptor's point of view (*e.g.*, the HGB area). As we will show in Section 4, the Gulf tracer can be used as a convenient indicator of clean maritime air masses to the Gulf Coast, which serves as a baseline to evaluate the ozone and $PM_{2.5}$ enhancements due to Central American fires. The two tracers were implemented in the model with a constant lifetime of 30 days, which resembles the lifetime of CO during the warm season.

The Gulf tracer is emitted at a constant rate per grid box (10^{-10} kg/m^2/s) from the Gulf of Mexico, and the fire tracer is emitted at the same rate from the grid boxes in Mexico and Central America that have at least one occurrence of fires during the study period. Figure S2 shows the source regions of the two tracers. The locations of the fires on a daily basis were derived from the Fire INventory from NCAR version 1.5 (FINN v1.5) (Wiedinmyer et al., 2011). We aggregated all the fire locations from the FINN during the study period into 0.5° × 0.5° grids and then re-gridded these locations onto the GEOS-Chem grids (0.5° × 0.625°). The tracer emission rate is not an important parameter, as the following analysis focuses on the relative spatiotemporal distribution of each tracer; that is, the absolute value of each tracer's mixing ratio is arbitrary and does not have a physical meaning.

Another important parameter for the fire tracer is fire injection height, which represents the vertical distribution of fire emissions near the source. The injection height is an important factor affecting the transport of fire emissions (Colarco et al., 2004; Kahn et al., 2008; Val Martin et al., 2010). Fire emissions that are injected in higher altitudes tend to have longer lifetime and wider spatial influences downwind (Freitas et al., 2006). The estimated injection height of Central American fires based on fireline intensity is around 0.9-1.5 km (Kauffman et al., 2003). Wang et al. (2006) used an injection height of 1.2 km in a regional model simulation of Central American fire emissions and tested the sensitivity of their model results to two different injection heights (1.0 km and 1.4 km). They found the differences in surface smoke concentrations in the southern U.S. between the sensitivity and baseline simulations to be within 15%. To represent the injection height of the fire tracer, we obtained the injection fraction of fire emissions over Mexico and Central America for April and May 2008 that were derived from MISR plume observations (Zhu et al., 2018). The MISR-derived injection fractions were initially at a resolution of 2° × 2.5°. The injection fraction for each grid was weighted by the grid's burned area to derive the regional-mean injection fraction over Central America. The regional-mean injection fraction (Figure S3) was used to redistribute the fire tracer emissions vertically for all the grids and the simulation periods. Overall, around 35% of the fire tracer emissions were above the estimated PBL (the 10th layer in the model, about 1.3 km), and 65% of the emissions remained within the PBL over Central America. If such injection height was not implemented (i.e. assuming all emissions were from the surface), fire tracer concentration over the HGB region would increase by 7% at the surface level but decrease by 4-13% between 0.5 and 3 km (Figure S4). This illustrates the importance of and sensitivity to the injection height. In this study, we do not consider the transport variability in injection height.

3. Transport pattern and mechanism

3.1 Transport patterns in the lower troposphere

Before discussing the influence of Central American fire emissions on the U.S. Gulf Coast, it is useful to present the transport patterns of the fire tracer in a broader perspective.

Figure 2a shows the spatial distribution of the fire tracer at 850 hPa averaged over the study period. The highest concentration is in the source regions as expected. The fire tracer is transported from the source region in two directions: southwestward toward the equator driven by the easterly winds near 10°N and north-/northwestward toward the U.S. Gulf Coast around the west edge of the Bermuda High whose center is located over Florida. Strong low-level winds are present on the west side of the anticyclone circulations, also known as the southerly low-level jet (SLLJ) (Doubler et al., 2015; Walters et al., 2008). The frequency of SLLJ is largest along the south Texas-northeast Mexico coastline, extending over the western Gulf of Mexico and the Yucatan coastline in April and May (Doubler et al., 2015; Sáenz & Durán-Quesada, 2015; Yu et al., 2017). This jet path coincides with the main transport pathways shown in the 14-year mean spatial distribution of the fire tracer (Figure 2a), indicating that the SLLJs are responsible for transporting Central American fire plumes to the U.S. Gulf Coast in the lower troposphere during springtime. Using the Hazard Mapping System (HMS) fire and smoke product, Kaulfus et al. (2017) showed large numbers of smoke occurrence days over the water in the northwestern Gulf of Mexico, indicative of Central America origin, and such features peak in the springtime and can extend to the Gulf coast under southerly winds. These features are reproduced in the GEOS-Chem simulation of the climatological distributions of the fire tracer from Central America to the U.S.

Figure 2b illustrates the vertical distribution of the fire tracer along the main transport route across the Gulf of Mexico (96.25-94.375°W; 18-30.5°N; the white box in Figure 2a). At the surface, the fire tracer decreases by 87% from its source region (~18°N) to the southern Texas coast (26-30.5°N). The transport within the boundary layer is mainly driven by low-level southerly winds. Compared to at the surface, the fire tracer mixing ratio decreases by 78%, 55%, 50% from the source region to the southern Texas coast at altitudes of 1.5, 3, and 6 km, respectively. The less reduction trend of fire tracer from the source to the receptor at higher altitudes implies that the influence of the fires on the U.S. Gulf Coast can extend vertically up to the middle troposphere where they can be more efficiently transported. Above the boundary layer, the fire tracer is first uplifted near the source region (~18-20°N), followed by subsidence from 3 km to the surface over the downwind region (28-30°N).

3.2 Transport mechanisms

The horizontal and vertical distributions of the fire tracer illustrate the mean transport patterns over the past fourteen years. However, the transport of fire emissions is episodic, and the associated air quality impact may depend more on the distribution of the large events. Wang et al. (2009) reported two cases in May 2003 with strong transport of Central American fire smoke toward the U.S. Gulf Coast, leading to moderate $PM_{2.5}$ levels (*e.g.*, $15.4 < PM_{2.5}$ mass < 40.4 μg m^{-3}) at several surface monitors in Texas and nearby regions. The transport of fire emissions in these cases was facilitated by the WCB, one primary airstream of a mid-latitude cyclone. The WCB originates in the warm sector of a mid-latitude cyclone, ascends from near surface, and brings large amounts of moisture up to the middle troposphere, facilitating formation of clouds and precipitation. WCB has been identified as a major mechanism exporting pollutants from one continent to another continent by lifting pollutants up to the free troposphere where they can be transported far downwind by stronger winds (Cooper et al., 2004; Cooper et al., 2002). Zhu et al. (2015) also indicated that the strong uplift in the WCB can make the pollutants produced in the fire plume rapidly reach to the free troposphere and the pollutants can be consequently transported further distances. Furthermore, precipitation associated with the WCB will remove the transported aerosols and soluble gases, which terminates the transport of Central American fires to the U.S (Wang et al., 2009).

Based on the above-mentioned literatures, and the 14-year mean transport patterns of the fire tracer, we present in Figure 3 a conceptual model of the transport pathways of fire emissions from Central America to the U.S. Gulf Coast. The main pathways include the SLLJs that are mainly responsible for transport within the PBL and the WCB associated with the mid-latitude cyclones for transport above the boundary layer. Other processes also participate in transport of fire emissions, such as subsidence from the middle troposphere, uplift from the surface or lower troposphere, and advection in the free troposphere. In terms of transport time scale for the main pathways, we estimated that it takes 1-2 days for air masses from Central America to the HGB region in the lower troposphere via the SLLJs based on the transport distance and mean wind speed. The transport time by the WCB from the boundary layer near Central America to the southern U.S. free troposphere is around 1 day (Wang et al., 2009). Next, we identify large transport events from the GEOS-Chem fire tracer distribution and examine if the variability of the large transport events can be explained by the SLLJs and/or WCBs pathways proposed in Figure 3. Compared to past studies, this study provides a quantitative long-term view for long-range transport events and their association with transport pathways including the LLJ and WCB in the conceptual model.

We define a meridional wind index (V_F) to represent the SLLJ intensity over the fire emission outflow region. The V_F index is calculated by averaging daily meridional wind speeds at 900 hPa over the Yucatan (red box in Figure 2a). The WCB events are selected by tracking the mid-latitude cyclones whose center appear in the eastern U.S. domain (29-50°N , 70-105°W) from the NSIDC database (Section 2.2) and the location of airstreams based on satellite cloud patterns (Carlson, 1980). Since not all mid-latitude cyclones identified in the domain would transport pollutants from Central American fires, we selected only those cyclones with cloud streams reaching Mexico and Central America using satellite images of the clouds from the Geostationary Operational Environmental Satellite (GOES).

The large transport events of the fire tracer are defined with respect to the impact over the HGB area, the largest metropolis on the Gulf Coast. For any given day during the study period, we extracted daily-mean fire tracer mixing ratio in each layer of the atmospheric column above the model grids containing the HGB area. If the enhancements of fire tracer mixing ratio at any level of the column exceed 75% compared to its 14-year average for that level, we labeled it as a large transport event. We categorized events according to their altitudes, defining an event as a surface event if it occurred at the surface (first model layer), as a "low-altitude" event if it occurred between 0-1.5 km (including surface events), or as a mid-altitude event if it occurred between 1.5-6 km. The altitude range for the low-altitude event is based on the averaged afternoon boundary layer over the HGB region in spring, which is around 1.5 km (Haman et al., 2014). The altitude range of the mid-altitude events (1.5-6 km) is based on the typical altitude range of the WCB from literature (Cooper et al., 2004; Liang et al., 2004). A day can be categorized into more than one types of events (*e.g.*, low-altitude and mid-altitude event) if the fire tracer profile over the HGB area meets more than one of the criteria listed above. We identified 403 mid-altitude events, 238 low-altitude events (including surface events), and 164 surface events during the study period. This corresponds to an average of 17 mid-altitude events, 9 low-altitude events (including surface events), and 6 surface events per month (April or May), respectively. Note those events were chosen solely based on the effect of transport, as there is no temporal variation in the fire tracer emissions in the model. There are 176 days categorized as both the low-altitude and mid-altitude events, representing 74% of the total low-altitude events and 44% of the total mid-altitude events. The high overlapping rates indicate that these two events are largely interconnected.

Figure 4 presents the number of the event days per year during the study period. The inter-annual variability of those events will be discussed in the next section. Considering the

study period as a whole, approximately 39% of the mid-altitude transport events (157 out of 403 mid-altitude events) overlap with the WCB events and 83% of the low-altitude events (197 out of 238 low-altitude events) have the V_F index larger than the 14-year mean. This verifies the conceptual model that the important mechanisms transporting fire emissions from Mexico and Central America to the HGB area are the WCBs through the mid-tropospheric route and the SLLJs through the low-tropospheric route. For the mid-altitude events, the WCBs may not be the dominant process, as only 39% of such events are associated with the WCBs. Other processes, such as advection in the free troposphere, may also contribute to the middle troposphere transport (Donnell et al., 2001). The low-altitude events appear to be dominated by the transport through the SLLJs. As shown in Figure S5, the low-altitude event days predominantly have higher values of the V_F index than other days (excluding low-altitude event days), which further supports our contention that strong SLLJs over the fire source region facilitate more efficient low-altitude transport of fire emissions from Central America to the U.S.

To better understand the relationship between the transport events and corresponding transport mechanisms, we separated the transport events into low-altitude only events (excluding those overlapped with mid-altitude events), mid-altitude only events (excluding those overlapped with low-altitude events), and overlapping events. Table 1 summarizes the number of each transport event associated with different transport mechanisms, including WCB only, SLLJ only, both WCB and SLLJ, and not either type. SLLJ-only is the dominant transport mechanism in the low altitude, accounting for 51% of the low-altitude only events. The majority of the mid-altitude only events are also related to the SLLJ near the source region, with 31.9% attributed to SLLJ-only pattern and 25% to SLLJ combined with WCB. Similarly, the majority of overlapping events are associated with SLLJ, with 43.3% to SSLJ-only and 44.3% to SSLJ combined with WCB. This implies that the dominant transport mechanism for the mid-latitude events (i.e. mid-altitude only and overlapping events) may be through the SLLJ transport followed by the WCB or other uplift mechanisms such as convection or large-scale upwelling. For the mid-altitude only events, the uplift may occur prior to the fire plume reaching the HGB region.

3.3 Interannual variability of transport events

Given the prevailing transport patterns we have identified, the transport of fire emissions from Central America to the U.S. occurs regularly every spring. However, the strength and magnitude of the transport vary. As demonstrated in Figure 4, there is indeed large inter-annual variability in the number of event days identified from the fire tracer simulation during the study period. For example, more transport events were found in 2003, 2008, and 2011, and fewer transport events in 2005, 2007, and 2012. In this section, we use the identified transport mechanisms to explain the year-to-year variability in the transport events.

In the lower troposphere, stronger SLLJs over the fire source region can enhance the transport of fire emissions from Central America to the U.S. Therefore, the intensity of SLLJ is expected to explain the inter-annual variability of the transport events in the lower troposphere. Figure 5a shows a strong correlation (r=0.83) between the V_F index and the number of all low-altitude events (low-altitude only and overlapping events). This suggests the intensity of SLLJs over the fire source region can explain 69% of the year-to-year variability in the number of the low-altitude transport events, according to the assumed linear relationship between the SLLJ intensity and the number of low-altitude events. When excluding the overlapping events, a lower correlation coefficient is found between the number of low-altitude only events and V_F index (r=0.35) (Figure S6a). This is because

76% of low-altitude events overlap with mid-altitude events and the majority of SLLJ-associated events are overlapping events (81 out of 176).

For the transport events in the middle troposphere, we focus on the role of the WCB. Given the results shown in Section 3.2, the WCB is an important but not the dominant mechanism transporting Central American fire emissions into the free troposphere. The number of the WCB events shows a moderate correlation of 0.56 with the number of all mid-altitude events (including overlapping events) (Figure 5b). This suggests that 31% of the total variation in the number of mid-altitude events can be explained by the assumed linear relationship with the number of WCB events. Excluding the overlapping events, the correlation of the mid-altitude events with the WCB does not change significantly ($r = 0.53$) (Figure S6b). This confirms the important role of the WCB to the mid-altitude events, although the WCB alone is not the dominant mechanism for this enhancement type (c.f. Table 1).

3.4 Transport case study

To further illustrate the transport mechanisms of the fire emissions, we analyzed a transport episode during 9-11 April 2008. This episode was chosen because there were large enhancements of the fire tracer in the lower and middle troposphere and offered an opportunity to further understand both the SLLJs and WCB transport mechanisms (Figure 6). Although strong transport was present from Central America to the U.S. during this event, we acknowledge that strong transport may or may not lead to pollution events depending on the intensity of fires. On April 9, there were two low-pressure systems in the mid-troposphere (700 hPa) centered at 43°N, 90°W (L1) and 38°N, 108°W (L2) respectively, building a meridional ridge line along 100°W north of 35°N (Figure 6a). The WCB associated with the L1 (WCB1) brought the fire tracer from the source region toward southern Texas in the middle troposphere; the WCB1 was captured by the GOES satellite imagery (Figure 6d). Similar patterns were also present in the lower troposphere, but in the lower troposphere it was the southerly flows over the Yucatan and the western Gulf of Mexico that brought the fire tracer toward southern Texas (Figure 6g). As shown in Figure 6j, CALIPSO captured transport of fire smokes from Mexico (~15°N) to southwestern Texas (~30-33°N) on April 9. The CALIPSO vertical feature mask shows an aerosol layer extending from the surface to 4 km from 15°N to 27°N and at 32°N (Figure 6j). CALIPSO-derived aerosol subtypes for that day indicate smoke mixed with maritime air from the source region to southwestern Texas at 2-4 km (Figure S7a). This is consistent with the fire tracer enhancement at the lower and middle troposphere from the GEOS-Chem model.

On the next day morning, April 10, the well-developed L2 moved eastward and replaced the ridge at 700 hPa. The WCB associated with the L2 (WCB2) was enhanced by the high-pressure system centered over Florida, leading to stronger transport of the fire tracer in the middle troposphere (Figure 6b) into the southern Great Plains (30-37°N, 90-100°W). This region did not show a large enhancement of the fire tracer in the lower troposphere, as the fire tracer was lifted up to the middle troposphere by the WCB2 (Figure 6h). The 'hot-spot' of the fire tracer in the lower troposphere was found in southwestern Texas due to the low-level transport by the SLLJs over the western Gulf of Mexico (Figure 6h).

During the early morning of April 11, as the L2 and WCB2 moved further northeastward, the fire tracer originally located over the southern US was further transported to the eastern U.S. at 700 hPa level (Figure 6c). At 850 hPa, the southerly flows associated with the mature high-pressure system over Florida (H) strengthened the SLLJs over the Yucatan and Gulf of Mexico. The strengthened SLLJs in combination with the anticlockwise flows around the low-level low-pressure center over northern Texas (L) enhanced and steered the transport of the fire tracer further to the western Gulf Coast and the southeastern U.S. in

the lower troposphere (Figure 6i). CALIPSO also identified transport of fire smoke from Central America (~18°N) to the HGB (~30°N) on April 11 (Figure 6k). The vertical feature mask presents an aerosol plume from 18°N to 30°N. The plume seems to be transported further north by a cloud stream at 28°N and mixed down to the boundary layer at 32°N (Figure 6k). The aerosol subtype plot shows signals of smoke aerosol at 2-4 km located at the receptor region (30-33°N) (Figure S7b). With this episode, we illustrated the important role of both SLLJs and WCB in transporting the fire tracer from Mexico and Central America to the U.S., which is captured by CALIPSO observations and consistent with the transport mechanisms and pathways in the conceptual model.

In addition to the transport case above demonstrating SLLJ and WCB transport mechanisms, another case on May 5, 2008 was chosen to present transport mechanism of advection in the free troposphere (Figure S8). This case had large enhancements of the fire tracer in the middle troposphere without the presence of the WCB. On this day, the fire tracer was transported northeastward from Mexico to southern Texas facilitated by large-scale winds over Mexico, a high-pressure center over the Gulf of Mexico, and a ridge over southern U.S. The enhancement of the fire tracer in the middle troposphere was caused by the predominantly horizontal and large-scale atmospheric flows, demonstrating the transport mechanism of advection.

4. Impact of Central American fires on air quality along the Gulf Coast

In this section, we estimate the impact of Central American fires on surface ozone and $PM_{2.5}$ over the HGB area and the Gulf Coast cities. Since the fire emissions and transport are highly episodic, the air quality impact is calculated only for a subset of the large transport events derived from the previous section. We use a compositing approach in which the composite of the identified transport events is compared with the composite of non-transport, baseline events in terms of the ozone and $PM_{2.5}$ levels at the receptors along the U.S. Gulf Coast. While case-to-case variability is not present in the composite, compositing a large number of transport events allows us to extract common features of air quality impact due to fire emissions.

4.1 Identification of fire-impact days

We have identified 164 surface transport events over the HGB area during the study period based on the fire tracer simulation (Section 3.2). However, since the tracer emissions did not change with time in the model, these events were selected solely by transport conditions, whereas in reality the magnitude of the fire emissions from Mexico and Central America is an important aspect affecting the impact of a transport event to the U.S. Here we used the data of daily total burned area from the FINN inventory which is derived from MODIS thermal anomalies to represent emission intensity over the source region and selected only the surface event days that had the burned area over Central America on the same day exceeding the 70^{th} percentile of the burned area distribution for the study period. The burned area data is retrieved from FINN over the source region that is delineated by longitude from 83.33 to 110°W, and by latitude from 10 to 26°N (black dashed domain in Figure 1). Those surface event days that meet the burned area criteria are referred to as the fire-impact days in the following sections. To establish a baseline condition for comparison with the fire-impact days, we sampled relatively clean days in a given receptor region (called clean-Gulf days) when the region predominantly receives clean maritime air masses from the Gulf of Mexico without contamination from the fire emissions. The clean-Gulf days were defined by the days meeting two conditions: (1) the enhancement of the Gulf tracer at the receptor grid is more

than 75% larger than the 14-year average, and (2) the burned area over Central America on the same day is lower than the 70th percentile of the burned area distribution. Using the 70th percentile cutoff for the burned area provides a sufficiently large and balanced sample size of the fire-impact days and the clean-Gulf days, which is 77 and 65 days for the HGB region respectively. If the 90th percentile of the burned area cutoff was used, the number of sampled fire-impact days decreased to 34 days and the number of clean-Gulf days increased to 104 days. However, the estimated ozone difference between the fire-impact and clean-Gulf days (see Section 4.3) changed by only 1.4% between the 70th and 90th percentile cutoff criteria for the burned area.

The fire-impact days and the clean-Gulf days are selected separately for individual receptors using the receptor-specific tracer concentrations. In addition to the HGB receptor, we selected an eastern Gulf Coast domain (red box in Figure 1) that covers several large cities along the Gulf Coast, including New Orleans in Louisiana, Mobile in Alabama, and Pensacola in Florida. We treated Corpus Christi as a separate receptor (blue box in Figure 1). Corpus Christi is more southerly than the other locations, and its coastline is parallel to the Mexican coastline; therefore, the wind pattern most favorable for transporting Central American fire emissions to Corpus Christi is mainly southerly, which is different from the southwesterly wind pattern required to transport Central American emissions to the eastern Gulf Coast cities. Therefore, Corpus Christi is not grouped with the eastern Gulf Coast cities.

Overall, the fire-impact days of the HGB identified by the criteria above account for 9% (77/854) of the whole study period, and the clean-Gulf days comprise 7.6% (65/854). The fire-impact days include all of the surface transport events with large fire emissions, and the clean-Gulf days comprise the baseline air masses that are predominantly influenced by clean maritime air. Before we compare the differences in ozone and $PM_{2.5}$ between the two composites, we sampled satellite data of CO and AOD during those days to establish that the two composites are indeed different in chemical composition.

4.2 Evidence from satellite observations

Satellite observations can be used to monitor the transport of fire emissions from a large-scale point of view and to validate the selections of fire-impact days and clean-Gulf days presented above. Although current satellites have the ability to retrieve ozone in the troposphere, it is difficult to measure ozone near the surface due to inadequate sensitivity of ozone within the boundary layer. As CO and AOD are commonly used tracers of fire emissions (Saide et al., 2015; Saide et al., 2016; Wang & Christopher, 2006; Wang, Christopher, et al., 2006; Wang et al., 2009), we sampled the satellite observations of CO and AOD during the HGB fire-impact days and the clean-Gulf days to verify if transport of fire emissions was detected by the satellite products. Figure 7a shows the daytime MOPITT total column CO observations averaged over ~~for~~ all the fire-impact days (77 days), all the clean-Gulf days (65 days), and the difference between the two. During the fire-impact days, the CO plume from Guatemala to Texas coastal cities can be seen impacting the coastal cities along the Gulf (*e.g.*, Corpus Christi and HGB), indicating transport of Central American fire plumes to the U.S. By comparison, during the clean-Gulf days, MOPITT sees much smaller CO signals over the fire source regions and CO tends to aggregate along the Mexican coast instead of spreading out. The total column enhancement of CO over the HGB region is around 2.8×10^{17} molec/cm^2, which is 13% higher compared to the clean-Gulf days.

Figure 7b presents the mean AOD from MODIS for all the fire-impact days (77 days), all the clean-Gulf days (65 days), and the difference between the two. During the fire-impact days, MODIS captures high AOD near the fire source region in Mexico and Central America with AOD enhancements from the source to the U.S. Gulf Coast, consistent with the transport pattern shown in Figure 2a and by other studies (Saide et al., 2015; Saide et al.,

2016). By contrast, during the clean-Gulf days, AOD near the source region is much less than that during the fire-impact days and minimal AOD enhancement is present along the transport route. AOD over the HGB area (red box in Figure 1) during the fire-impact days is higher by 0.24 or 29% higher compared to the clean-Gulf days. As the CO from MOPITT is also enhanced during the fire-impact days (Figure 7a), the AOD enhancement is not likely mainly due to dust. However, AOD is enhanced more than CO, which may be explained by aerosols that are not co-emitted with CO (such as dust) as well as secondary aerosol (such as industrial emissions) which are found to be important sources of $PM_{2.5}$ in Mexico (Martínez-Cinco et al., 2016). The simultaneous enhancements of both CO and AOD during the fire-impact days could also be caused by the mixture of anthropogenic air pollution from Mexico and Central America with the fire emissions. Overall, the analysis of satellite observations of CO and AOD gives confidence in the selection of the fire-impact days and clean-Gulf days.

4.3 Ozone and $PM_{2.5}$ enhancement on the Gulf Coast due to fires

We expect to find a difference in background ozone between the fire-impact days and clean-Gulf days at the receptor regions, as both types of days are defined with respect to non-local air masses and background ozone represents the influence of outside sources to a receptor. Only the HGB region has background ozone data (Berlin et al., 2011). Figure 8a shows the box plot of HGB background ozone for the fire-impact days, clean-Gulf days, and the whole study period. The fire-impact days have relatively higher background ozone, ranging from 18 ppbv to 60 ppbv, compared to background ozone from the clean-Gulf days which ranges from 11 ppbv to 42 ppbv (Figure 8a). The difference in the mean background ozone between the two composite groups is 7.0 ± 1.4 ppbv, and this difference is statistically significant ($p < 0.05$) based on the two-sample t-test. Background ozone during the fire-impact days and clean-Gulf days is both lower than the mean background ozone over the study period. This is because the HGB is also influenced by the polluted continental air masses from the north which typically have higher background ozone than the southerly air masses coming from the Gulf of Mexico. Based on emissions inventories for Central Mexico by Emmons et al. (2010), open fire emissions account for at least 40% of total annual emissions of VOCs, OC, BC, and CO from Central America. Since fire emissions happen predominantly in spring, we expect the fire emissions to dominate in the total emissions in this season, although we acknowledge that the differences of background ozone between fire-impact days and clean-Gulf days may include the influence of anthropogenic emissions from Central America transported together with fire emissions.

Figure 8b presents the box plot comparison of MDA8 ozone distribution for the fire-impact days and clean-Gulf days over the HGB and other Gulf Coast cities. Table 2 summarizes the number of fire-impact days and clean-Gulf days, and the mean difference in MDA8 ozone mixing ratio between the two composite groups for each city. The number of fire-impact days decreases from west to east along the Gulf Coast (*i.e.*, decreasing from Corpus Christi to HGB and to the eastern Gulf Coast cities), which is consistent with the transport pathways discussed above, indicating that the probability of being influenced by Central American fire emissions would decrease as the distance from Central America increases. Compared to the corresponding clean-Gulf days, the mean MDA8 ozone enhancement during the fire-impact days is 11.9 ± 1.6, 9.7 ± 1.7, 2.7 ± 1.6, 4.3 ± 1.6, and 4.6 ± 1.7 ppbv for Corpus Christi, HGB, New Orleans, Mobile, and Pensacola, respectively. Note these enhancements are averages over the selected transport events (*i.e.*, episodes), instead of over the whole study period. As such, they indicate the average ozone increase at those cities that can be attributed to episodic transport of fire and anthropogenic emissions from Mexico and Central America. Among all the cities examined, Corpus Christi has the largest ozone

enhancement. This can be partly explained by the fact that Corpus Christi is located closest to Mexico which is the large fire source region.

As discussed in Section 3.2, it typically takes 1-2 days transport time from Central America to the Gulf Coast. If the burned area one day before was used to sample fire-impact days and clean-Gulf days, the differences in calculated number of days and estimated enhancement of pollutant level are small and not statistically insignificant, as shown in Table S1. Therefore, our results are not sensitive to the choice of burned area on the same day or the day before.

The HGB region has the second largest MDA8 ozone enhancement (9.7 ± 1.7 ppbv) among the Gulf Coast cities, which could be partly explained by its closer location relative to the source region than other cities. The average MDA8 ozone over the HGB region is 45 ppbv for the study period (Apr and May). Given the current ozone standard of 70 ppbv, an addition of 9.7 ppbv from Central American fires would not significantly affect the nonattainment statistics in the HGB region. Indeed, there is only one ozone exceedance day (79 ppbv, on May 18, 2003) among the fire-impact days for the HGB region. The MDA8 ozone enhancement at the HGB is about 2.7 ppbv larger than the background ozone enhancement. This difference might represent the potential perturbation of ozone production from local emissions by fire and anthropogenic pollutions transport from Central America. Using a novel statistical method (generalized additive model), Gong et al. (2017) estimated an average 8.1 ppbv enhancement of ozone in Houston due to fires during the period of May-September 2008-2015. They identified the fire events based on the combination of the HMS Fire and Smoke Products and surface $PM_{2.5}$ observations, and as such the fire events considered in their analysis include both domestic fires and those transported over long distances from Central America. Our estimate of the ozone enhancement in Houston due to Central America fires alone is 9.7 ± 1.7 ppbv, which is slightly higher than the estimation by Gong et al. (2017). The difference in the two estimates can be attributed to the differences in the approach, study period, and baseline selection. For example, Gong et al. (2017) includes summertime when the westward shift of the Bermuda High brings clean maritime air into the HGB region and leads to lower ozone (Wang et al., 2016). Therefore, we would expect lower ozone enhancement in Gong et al. (2017) than our study that focuses only on springtime.

Using the similar approach to ozone, we sampled the $PM_{2.5}$ observations for the fire-impact days and clean-Gulf days for each city and estimated the impact of Central American fires on $PM_{2.5}$ air quality along the Gulf Coast. The results are shown in Figure 9. Compared with the corresponding clean-Gulf days, the mean $PM_{2.5}$ enhancement during the fire-impact days is 4.7 ± 1.1, 3.9 ± 1.7, 2.1 ± 0.7, 3.6 ± 0.8, and 2.8 ± 0.8 $\mu g/m^3$ for Corpus Christi, HGB, New Orleans, Mobile, and Pensacola, respectively. Note that the number of $PM_{2.5}$ data is smaller for Mobile due to the limited observation frequency. Based on concurrent sampling of surface $PM_{2.5}$ monitors with the HMS Fire and Smoke Products, Kaulfus et al. (2017) reported around 3-8 $\mu g/m^3$ enhancements of $PM_{2.5}$ over the urban areas along the Gulf Coast by wildfires during springtime (March-May) 2005-2016. The enhancements that we calculated are in the range of their estimate but on the lower side. The estimate by Kaulfus et al. (2017) includes not only the influence of Central American fires but also the domestic fires (e.g. biomass burning in Kansas), leading to larger enhancements compared to our estimate. Our results suggest a 22.5% increase of $PM_{2.5}$ for New Orleans, Louisiana, which is in line with a 29% enhancement from Wang et al. (2006) for a transport case to Louisiana in 2003. Tanner et al. (2001) analyzed another case for Mar-May 1998 and showed 386% and 181% increases of mean $PM_{2.5}$ over Tennessee and Arkansas due to transport of fire emissions from Central America, which is much higher than our estimation of 22%-43% average $PM_{2.5}$ enhancements for the Gulf Coast cities. This difference may be explained by

the fact that fires in 1998 was the largest and abnormal event in record which was not included in our study period.

Besides the differences in fire emissions, the fire-impact days and clean-Gulf days may also differ in some meteorological factors affecting ozone and PM formation. For example, maritime flows would result in abundant water vapor in the atmosphere and increase morning low cloud fraction over the HGB (Day et al., 2010). Figure S9 compares the distributions of several meteorological factors over the HGB region between the fire-impact days and clean-Gulf days. Significant differences (p-value < 0.05) between the two groups are found in all meteorological factors except for precipitation. The fire-impact days on average tend to have higher temperature, lower relative humidity (RH), and lower cloud fraction that would promote ozone production from the fire emissions. In terms of wind speed and direction, strong southerly and easterly winds are found during the clean-Gulf days. The differences of meteorological factors in the groups of fire-impact days and clean-Gulf days suggest that the differences in meteorological factors such as temperature, RH, and clouds also contribute to the quantified impact of fires on ozone and PM air quality.

5. Conclusion

We integrated satellite observations, ground measurements, and modeling to develop the springtime climatology of transport pathways of Central American fire emissions to the U.S. Gulf Coast over a long-term period (2002-2015) and estimated the contribution of pollutants from fires on surface ozone and $PM_{2.5}$ in the urban areas along the Gulf Coast. We conducted a GEOS-Chem passive tracer simulation by using the fire tracer and the Gulf tracer to track the transport of fire-polluted air and clean maritime air to the Gulf Coast. A conceptual model is presented to generalize the transport mechanisms of the fire emissions, which include the strong southerly winds (*i.e.*, SLLJs) that are mainly responsible for transport within the boundary layer and the WCB of mid-latitude cyclones for transport above the boundary layer.

We identified the large transport events during the study period from the GEOS-Chem fire tracer distribution: the monthly average occurrence for April or May of those large transport events was 17, 9, and 6 in the middle and lower troposphere and at the surface, respectively. Approximately 39% of all mid-altitude events (mid-only and overlapping events) occurred through the WCBs (157 out of 403 mid-altitude events) and 83% of all low-altitude events (low-only and overlapping events) were related to SLLJs, defined as V_F intensity being larger than the 14-year mean intensity (197 out of 238 low-altitude events). The inter-annual variability of the large transport events can be also explained by the SLLJs and/or WCBs. The number of low-altitude events shows a significant correlation of 0.83 with the SLLJ intensity (*i.e.*, V_F index), and the number of mid-altitude events exhibits a moderate correlation of 0.56 with the number of WCB events. These findings strengthen our conceptual model of the transport mechanisms and demonstrate the influence of the meteorological mechanisms on the year-to-year variability in transported fire emissions.

The fire-impact days and clean-Gulf days were identified by considering both transport and emissions. For the HGB, the largest metropolis on the Gulf Coast, the composite of the fire-impact days has a higher background ozone by 7.0 ± 1.4 ppbv and higher MDA8 ozone by 9.7 ± 1.7 ppbv, compared to the composite of the clean-Gulf days. Only one ozone exceedance day (79 ppbv, on May 18, 2003) was found among the fire-impact days for the HGB region. For other Gulf Coast cities examined here, the MDA8 ozone enhancement in the fire-impact composite ranges between 2.7 to 11.9 ppbv. The composite of the fire-impact days has higher $PM_{2.5}$ concentrations by 2-5 $\mu g/m^3$ compared to the clean-Gulf composite. While the estimated ozone and $PM_{2.5}$ enhancements are all statistically

significant, they likely include contributions from anthropogenic emissions over the fire source regions, as the fire emissions may be mixed with other emissions (*e.g*., transportation, industrial, and residential) in Mexico and Central America and the composite approach taken here does not separate them. However, since the fire-impact days have predominantly larger burned areas (higher than 70th-percentile of the distribution), the contribution of fire emissions likely dominates. Satellite observations of CO and AOD show a significant increase in CO (13%) and AOD (19%) over the HGB area during the selected fire-impact days compared to the clean-Gulf days, lending support to our selection of fire-impact days and clean-Gulf days.

The present work focuses on the meteorological mechanisms that drive the large transport events as well as their inter-annual variability and uses those meteorologically-favorable transport events to form the sampling basis to estimate the impact of Central America fire emissions on ozone and $PM_{2.5}$ air quality for the Gulf Coast cities. The compositing approach does not examine the case-by-case variability. Therefore, we do not explicitly examine other internal factors affecting the fire impact on air quality, such as the chemical evolution of fire-emitted species and ozone precursors during the course of the plume transport and mixture of the fire emissions with urban pollution (Baylon et al., 2018). Future work is needed to improve our understanding of these aspects, which would require in-situ measurements of the fire plumes as well as detailed modeling of the plume chemistry and small-scale transport.

Acknowledgements:

The authors acknowledge the European Centre for Medium-Range Weather Forecasts (ECMWF) for providing the ERA-Interim reanalysis data, NASA Langley Research Center for CALIPSO data, MOPITT science team for MOPITT data, and MODIS science team for MODIS AOD data. This work was funded by a grant from the Texas Air Quality Research Program (AQRP 16-008) at The University of Texas at Austin through the Texas Emission Reduction Program (TERP) and the Texas Commission on Environmental Quality (TCEQ). The findings, opinions, and conclusions are the work of the authors and do not necessarily represent findings, opinions, or conclusions of the AQRP or the TCEQ. The authors thank the University of Houston Center for Advanced Computing and Data Science (CACDS) for providing computational resources.

References

Andreae, M. O., & Merlet, P. (2001). Emission of trace gases and aerosols from biomass burning. *Global biogeochemical cycles*, 15(4), 955-966.

Baylon, P., Jaffe, D., Hall, S., Ullmann, K., Alvarado, M., & Lefer, B. (2018). Impact of Biomass Burning Plumes on Photolysis Rates and Ozone Formation at the Mount Bachelor Observatory. *Journal of Geophysical Research: Atmospheres*, 123(4), 2272-2284. doi:10.1002/2017JD027341

Berlin, S. R., Langford, A. O., Estes, M., Dong, M., & Parrish, D. D. (2013). Magnitude, decadal changes, and impact of regional background ozone transported into the greater Houston, Texas, Area. *Environmental science & technology*, 47(24), 13985-13992.

Carlson, T. N. (1980). Airflow through midlatitude cyclones and the comma cloud pattern. *Monthly Weather Review*, 108(10), 1498-1509.

Colarco, P., Schoeberl, M., Doddridge, B., Marufu, L., Torres, O., & Welton, E. (2004). Transport of smoke from Canadian forest fires to the surface near Washington, DC: Injection height, entrainment, and optical properties. *Journal of Geophysical Research: Atmospheres*, 109(D6). D06203. doi:10.1029/2003JD004248

Cooper, O., Forster, C., Parrish, D., Trainer, M., Dunlea, E., Ryerson, T., et al. (2004). A case study of transpacific warm conveyor belt transport: Influence of merging airstreams on trace gas import to North America. *Journal of Geophysical Research: Atmospheres*, 109(D23). D23S08. doi:10.1029/2003JD003624

Cooper, O., Moody, J., Parrish, D., Trainer, M., Ryerson, T., Holloway, J., et al. (2002). Trace gas composition of midlatitude cyclones over the western North Atlantic Ocean: A conceptual model. *Journal of Geophysical Research: Atmospheres*, 107(D7). 4056. doi:10.1029/2001JD000901

Crutzen, P. J., & Andreae, M. O. (1990). Biomass burning in the tropics: Impact on atmospheric chemistry and biogeochemical cycles. *Science*, 250(4988), 1669-1678.

Davis, R. E., Hayden, B. P., Gay, D. A., Phillips, W. L., & Jones, G. V. (1997). The north atlantic subtropical anticyclone. *Journal of Climate*, 10(4), 728-744.

Day, B. M., Rappenglück, B., Clements, C. B., Tucker, S. C., & Brewer, W. A. (2010). Nocturnal boundary layer characteristics and land breeze development in Houston, Texas during TexAQS II. *Atmospheric environment*, 44(33), 4014-4023.

Deeter, M., Edwards, D., Gille, J., & Drummond, J. R. (2007). Sensitivity of MOPITT observations to carbon monoxide in the lower troposphere. *Journal of Geophysical Research: Atmospheres*, 112(D24). D24306. doi:10.1029/2007JD008929

Deeter, M., Edwards, D., Gille, J., & Drummond, J. R. (2009). CO retrievals based on MOPITT near-infrared observations. *Journal of Geophysical Research: Atmospheres*, 114(D4). D04303. doi:10.1029/2008JD010872

Deeter, M. N., Edwards, D. P., Francis, G. L., Gille, J. C., Martínez-Alonso, S., Worden, H. M., & Sweeney, C. (2017). A climate-scale satellite record for carbon monoxide: the MOPITT Version 7 product. *Atmospheric Measurement Techniques*, 10(7), 2533.

Dirksen, R. J., Folkert Boersma, K., De Laat, J., Stammes, P., Van Der Werf, G. R., Val Martin, M., & Kelder, H. M. (2009). An aerosol boomerang: Rapid around-the-world transport of smoke from the December 2006 Australian forest fires observed from space. *Journal of Geophysical Research: Atmospheres*, 114(D21). D21201. doi:10.1029/2009JD012360

Donnell, E. A., Fish, D. J., Dicks, E. M., & Thorpe, A. J. (2001). Mechanisms for pollutant transport between the boundary layer and the free troposphere. *Journal of Geophysical Research: Atmospheres*, 106(D8), 7847-7856. doi:10.1029/2000JD900730

Doubler, D. L., Winkler, J. A., Bian, X., Walters, C. K., & Zhong, S. (2015). An NARR-Derived Climatology of Southerly and Northerly Low-Level Jets over North America and Coastal Environs. *Journal of Applied Meteorology and Climatology*, 54(7), 1596-1619.

Emmons, L., Apel, E., Lamarque, J.-F., Hess, P., Avery, M., Blake, D., et al. (2010). Impact of Mexico City emissions on regional air quality from MOZART-4 simulations. *Atmospheric Chemistry and Physics*, 10(13), 6195-6212.

Fiore, A. M., Jacob, D. J., Bey, I., Yantosca, R. M., Field, B. D., Fusco, A. C., & Wilkinson, J. G. (2002). Background ozone over the United States in summer: Origin, trend, and contribution to pollution episodes. *Journal of Geophysical Research: Atmospheres*, 107(D15). 4275. doi:10.1029/2001JD000982

Freitas, S., Longo, K., & Andreae, M. (2006). Impact of including the plume rise of vegetation fires in numerical simulations of associated atmospheric pollutants. *Geophysical research letters*, 33(17). L17808. doi:10.1029/2006GL026608

Gong, X., Kaulfus, A., Nair, U., & Jaffe, D. A. (2017). Quantifying O3 Impacts in Urban Areas Due to Wildfires Using a Generalized Additive Model. *Environmental science & technology*, 51(22), 13216-13223.

Hall, E., Beaver, M., Long, R. W., & Vanderpool, R. W. (2012). EPA's Reference and Equivalent Supporting NAAQS Implementation through Methods Research Program: Research, Development, and Analysis., from Air & Waste Management Association

Haman, C., Couzo, E., Flynn, J., Vizuete, W., Heffron, B., & Lefer, B. (2014). Relationship between boundary layer heights and growth rates with ground-level ozone in Houston, Texas. *Journal of Geophysical Research: Atmospheres*, 119(10), 6230-6245. doi:10.1002/2013JD020473

Huang, J., Minnis, P., Chen, B., Huang, Z., Liu, Z., Zhao, Q., et al. (2008). Long-range transport and vertical structure of Asian dust from CALIPSO and surface measurements during PACDEX. *Journal of Geophysical Research: Atmospheres*, 113(D23). D23212. doi:10.1029/2008JD010620

Jaffe, D., Bertschi, I., Jaeglé, L., Novelli, P., Reid, J. S., Tanimoto, H., et al. (2004). Long-range transport of Siberian biomass burning emissions and impact on surface ozone in western North America. *Geophysical research letters*, 31(16). L16106. doi:10.1029/2004GL020093

Kahn, R. A., Chen, Y., Nelson, D. L., Leung, F. Y., Li, Q., Diner, D. J., & Logan, J. A. (2008). Wildfire smoke injection heights: Two perspectives from space. *Geophysical research letters*, 35(4). L04809. doi:10.1029/2007GL032165

Kauffman, J., Steele, M., Cummings, D., & Jaramillo, V. (2003). Biomass dynamics associated with deforestation, fire, and, conversion to cattle pasture in a Mexican tropical dry forest. *Forest Ecology and Management*, 176(1-3), 1-12.

Kaulfus, A. S., Nair, U., Jaffe, D., Christopher, S. A., & Goodrick, S. (2017). Biomass Burning Smoke Climatology of the United States: Implications for Particulate Matter Air Quality. *Environmental science & technology*, 51(20), 11731-11741.

Kleindienst, T. E., Hudgens, E. E., Smith, D. F., McElroy, F. F., & Bufalini, J. J. (1993). Comparison of chemiluminescence and ultraviolet ozone monitor responses in the presence of humidity and photochemical pollutants. *Air & Waste*, 43(2), 213-222.

Koren, I., Kaufman, Y. J., Remer, L. A., & Martins, J. V. (2004). Measurement of the effect of Amazon smoke on inhibition of cloud formation. *Science*, 303(5662), 1342-1345.

Leung, F. Y. T., Logan, J. A., Park, R., Hyer, E., Kasischke, E., Streets, D., & Yurganov, L. (2007). Impacts of enhanced biomass burning in the boreal forests in 1998 on tropospheric chemistry and the sensitivity of model results to the injection height of emissions. *Journal of Geophysical Research: Atmospheres*, 112(D10). D10313. doi:10.1029/2006JD008132

Liang, Q., Jaeglé, L., Jaffe, D. A., Weiss-Penzias, P., Heckman, A., & Snow, J. A. (2004). Long-range transport of Asian pollution to the northeast Pacific: Seasonal variations and transport pathways of carbon monoxide. *Journal of Geophysical Research: Atmospheres*, 109(D23). D23S07. doi:10.1029/2003JD004402

Liu, Z., Omar, A., Vaughan, M., Hair, J., Kittaka, C., Hu, Y., et al. (2008). CALIPSO lidar observations of the optical properties of Saharan dust: A case study of long-range transport. *Journal of Geophysical Research: Atmospheres*, 113(D7). D07207. doi:10.1029/2007JD008878

Logan, T., Dong, X., & Xi, B. (2018). Aerosol properties and their impacts on surface CCN at the ARM Southern Great Plains site during the 2011 Midlatitude Continental Convective Clouds Experiment. *Advances in Atmospheric Sciences*, 35(2), 224-233.

Lu, X., Zhang, L., Xu, Y., Zhang, J., Jaffe, D. A., Stohl, A., et al. (2016). Wildfire influences on the variability and trend of summer surface ozone in the mountainous western United States. *Atmospheric Chemistry and Physics*, 16(22), 14687.

Martínez-Cinco, M., Santos-Guzmán, J., & Mejía-Velázquez, G. (2016). Source apportionment of PM2. 5 for supporting control strategies in the Monterrey Metropolitan Area, Mexico. *Journal of the Air & Waste Management Association*, 66(6), 631-642.

McDonald-Buller, E. C., Allen, D. T., Brown, N., Jacob, D. J., Jaffe, D., Kolb, C. E., et al. (2011). Establishing policy relevant background (PRB) ozone concentrations in the United States. *Environmental science & technology*, 45(22), 9484-9497.

Mendoza, A., Garcia, M. R., Vela, P., Lozano, D. F., & Allen, D. (2005). Trace gases and particulate matter emissions from wildfires and agricultural burning in Northeastern Mexico during the 2000 fire season. *Journal of the Air & Waste Management Association*, 55(12), 1797-1808.

Miller, D. J., Sun, K., Zondlo, M. A., Kanter, D., Dubovik, O., Welton, E. J., et al. (2011). Assessing boreal forest fire smoke aerosol impacts on US air quality: A case study using multiple data sets. *Journal of Geophysical Research: Atmospheres*, 116(D22). D22209. doi:10.1029/2011JD016170

MOPITT Science Team. (2013). MOPITT/Terra Level 3 Gridded Daily CO (on a latitude/longitude/pressure grid) derived from Near and Thermal Infrared Radiances (Publication no. 10.5067/TERRA/MOPITT/MOP03J_L3.007). from NASA Atmospheric Science Data Center (ASDC)

Park, R. J., Jacob, D. J., Chin, M., & Martin, R. V. (2003). Sources of carbonaceous aerosols over the United States and implications for natural visibility. *Journal of Geophysical Research: Atmospheres*, 108(D12). 4355. doi:10.1029/2002JD003190

Parrish, D., Millet, D., & Goldstein, A. (2009). Increasing ozone in marine boundary layer inflow at the west coasts of North America and Europe. *Atmospheric Chemistry and Physics*, 9(4), 1303-1323.

Peppler, R., Bahrmann, C., Barnard, J. C., Laulainen, N., Turner, D., Campbell, J., et al. (2000). ARM Southern Great Plains site observations of the smoke pall associated with the 1998 Central American fires. *Bulletin of the American Meteorological Society*, 81(11), 2563-2591.

Platnick, S., King, M. D., Meyer, K. G., Wind, G., Amarasinghe, N., Marchant, B., et al. (2014). MODIS cloud optical properties: User guide for the Collection 6 Level-2 MOD06/MYD06 product and associated Level-3 Datasets. *Version 0.9 (beta)*, 17.

Regener, V. H. (1964). Measurement of atmospheric ozone with the chemiluminescent method. *Journal of Geophysical Research*, 69(18), 3795-3800.

Reid, J., Koppmann, R., Eck, T., & Eleuterio, D. (2005). A review of biomass burning emissions part II: intensive physical properties of biomass burning particles. *Atmospheric Chemistry and Physics*, 5(3), 799-825.

Remer, L. A., Kaufman, Y., Tanré, D., Mattoo, S., Chu, D., Martins, J. V., et al. (2005). The MODIS aerosol algorithm, products, and validation. *Journal of the Atmospheric Sciences*, 62(4), 947-973.

Rogers, C. M., & Bowman, K. P. (2001). Transport of smoke from the Central American fires of 1998. *Journal of Geophysical Research: Atmospheres*, 106(D22), 28357-28368. doi:10.1029/2000JD000187

Sáenz, F., & Durán-Quesada, A. M. (2015). A climatology of low level wind regimes over Central America using a weather type classification approach. *Frontiers in Earth Science*, 3(15). doi:10.3389/feart.2015.00015

Saide, P., Spak, S., Pierce, R., Otkin, J., Schaack, T., Heidinger, A., et al. (2015). Central American biomass burning smoke can increase tornado severity in the US. *Geophysical research letters*, 42(3), 956-965. doi:10.1002/2014GL062826

Saide, P., Thompson, G., Eidhammer, T., Silva, A. M., Pierce, R. B., & Carmichael, G. R. (2016). Assessment of biomass burning smoke influence on environmental conditions for multiyear tornado outbreaks by combining aerosol-aware microphysics and fire emission constraints. *Journal of Geophysical Research: Atmospheres*, 121(17), 10294-10311. doi:10.1002/2016JD025056

Sinha, P., Jaeglé, L., Hobbs, P. V., & Liang, Q. (2004). Transport of biomass burning emissions from southern Africa. *Journal of Geophysical Research: Atmospheres*, 109(D20). D20204. doi:10.1029/2004JD005044

Tanner, R. L., Parkhurst, W. J., Valente, M. L., Humes, K. L., Jones, K., & Gilbert, J. (2001). Impact of the 1998 Central American fires on PM2. 5 mass and composition in the southeastern United States. *Atmospheric environment*, 35(36), 6539-6547.

Val Martin, M., Logan, J., Kahn, R., Leung, F., Nelson, D., & Diner, D. (2010). Smoke injection heights from fires in North America: analysis of 5 years of satellite observations. *Atmospheric Chemistry and Physics*, 10(4), 1491-1510.

Walters, C. K., Winkler, J. A., Shadbolt, R. P., van Ravensway, J., & Bierly, G. D. (2008). A long-term climatology of southerly and northerly low-level jets for the central United States. *Annals of the Association of American Geographers*, 98(3), 521-552.

Wang, J., & Christopher, S. A. (2006). Mesoscale modeling of Central American smoke transport to the United States: 2. Smoke radiative impact on regional surface energy budget and boundary layer evolution. *Journal of Geophysical Research: Atmospheres*, 111(D14). D14S92. doi:10.1029/2005JD006720

Wang, J., Christopher, S. A., Nair, U., Reid, J. S., Prins, E. M., Szykman, J., & Hand, J. L. (2006). Mesoscale modeling of Central American smoke transport to the United States: 1."Top-down" assessment of emission strength and diurnal variation impacts. *Journal of Geophysical Research: Atmospheres*, 111(D5). D05S17. doi:10.1029/2005JD006416

Wang, J., Van den Heever, S. C., & Reid, J. S. (2009). A conceptual model for the link between Central American biomass burning aerosols and severe weather over the south central United States. *Environmental Research Letters*, 4(1), 015003. doi:10.1088/1748-9326/4/1/015003.

Wang, Y., Jia, B., Wang, S.-C., Estes, M., Shen, L., & Xie, Y. (2016). Influence of the Bermuda High on interannual variability of summertime ozone in the Houston–Galveston–Brazoria region. *Atmospheric Chemistry and Physics*, 16(23), 15265-15276.

Wiedinmyer, C., Akagi, S., Yokelson, R. J., Emmons, L., Al-Saadi, J., Orlando, J., & Soja, A. (2011). The Fire INventory from NCAR (FINN): a high resolution global model to estimate the emissions from open burning. *Geoscientific Model Development*, 4(3), 625.

Winker, D., Pelon, J., Coakley Jr, J., Ackerman, S., Charlson, R., Colarco, P., et al. (2010). The CALIPSO mission: A global 3D view of aerosols and clouds. *Bulletin of the American Meteorological Society*, 91(9), 1211-1230.

Worden, H., Deeter, M., Edwards, D., Gille, J., Drummond, J., & Nédélec, P. (2010). Observations of near-surface carbon monoxide from space using MOPITT

multispectral retrievals. *Journal of Geophysical Research: Atmospheres*, 115(D18). D18314. doi:10.1029/2010JD014242

Yokelson, R. J., Crounse, J., DeCarlo, P., Karl, T., Urbanski, S., Atlas, E., et al. (2009). Emissions from biomass burning in the Yucatan. *Atmospheric Chemistry and Physics*, 9(15), 5785.

Yu, L., Zhong, S., Winkler, J. A., Doubler, D. L., Bian, X., & Walters, C. K. (2017). The inter-annual variability of southerly low-level jets in North America. *International Journal of Climatology*, 37(1), 343-357.

Zhang, L., Jacob, D. J., Downey, N. V., Wood, D. A., Blewitt, D., Carouge, C. C., et al. (2011). Improved estimate of the policy-relevant background ozone in the United States using the GEOS-Chem global model with 1/2× 2/3 horizontal resolution over North America. *Atmospheric environment*, 45(37), 6769-6776.

Zhu, L., Fischer, E. V., Payne, V. H., Worden, J. R., & Jiang, Z. (2015). TES observations of the interannual variability of PAN over Northern Eurasia and the relationship to springtime fires. *Geophysical research letters*, 42(17), 7230-7237. doi:10.1002/2015GL065328

Zhu, L., Martin, M. V., Hecobian, A., Gatti, L. V., Kahn, R., & Fischer, E. V. (2018). Development and implementation of a new biomass burning emissions injection height scheme for the GEOS-Chem model. *Geosci. Model Dev. Discuss.* doi:10.5194/gmd-2018-93, in review, 2018.

Table 1. The number of each type of enhancement and association with the transport types. The percentage refers to the relative contribution of a given transport pattern to each type of HGB enhancement events.

Transport mechanism / HGB event type	WCB	SLLJ	Both	Not either	Total
Low-altitude only event	2 (4%)	26 (51%)	7 (13.7%)	16 (31.3%)	59 (100%)
Mid-altitude only event	19 (8.8%)	69 (31.9%)	54 (25%)	74 (34.2%)	216 (100%)
Overlapping event	1 (0.5%)	81 (43.3%)	83 (44.3%)	22 (11.7%)	187 (100%)

Table 2. The number of fire-impact days and clean-Gulf days for the Gulf Coast cities for the study period of April and May 2002-2015 (854 days) and the estimated MDA8 ozone and $PM_{2.5}$ enhancement by Central American fires.

	Corpus Christi	HGB	New Orleans	Mobile	Pensacola
Number of fire-impact days	88	77	59	59	59
Number of clean-Gulf days	49	65	114	114	114
MDA8 ozone enhancement by fires (ppbv)	11.9 ± 1.6	9.7 ± 1.7	2.7 ± 1.55	4.3 ± 1.6	4.6 ± 1.7
$PM_{2.5}$ enhancement by fires ($\mu g/m^3$)	4.7 ± 1.1	3.9 ± 0.9	2.1 ± 0.7	3.6 ± 0.8	2.8 ± 0.8

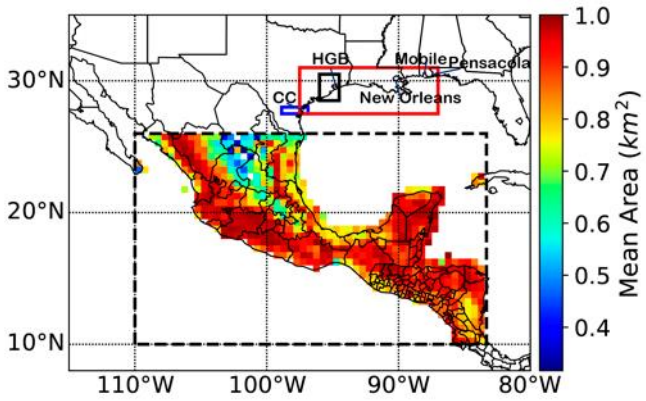

Figure 1. Locations of Corpus Christi (CC, blue box; 96.87-98.87°W; 27.5-28°N), the HGB region (solid black box; 94.5-96°W; 28.5-30.5°N), the eastern Gulf Coast (red box; 87-97.5°W; 27.5-31°N), and the fire source region for retrieving burned area (dashed black box; 83.33-110°W; 10-26°N). The colored grid boxes show the averaged burned area for April and May 2002-2015 from the Fire INventory from NCAR version 1.5 (FINNv1.5).

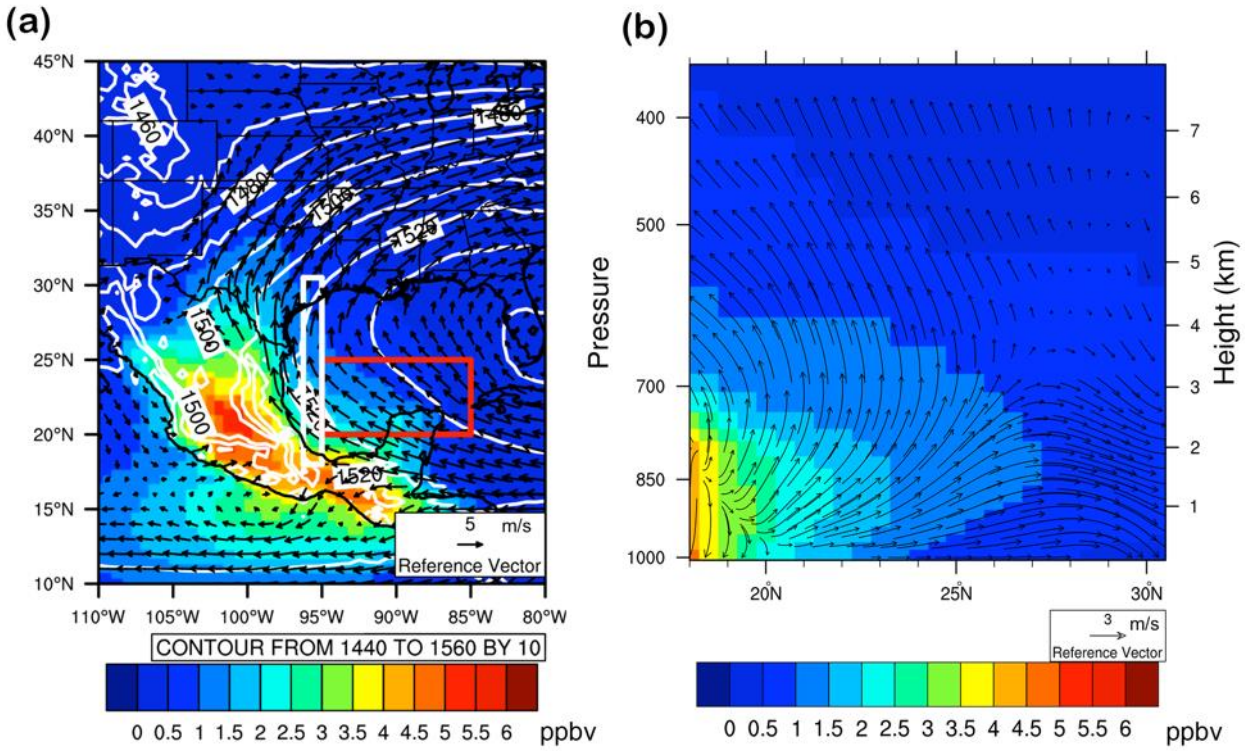

Figure 2. (a) Mean spatial distribution of the fire tracer for the time period of April and May 2002-2015 at 850 hPa. The red box (85-95°W, 20-25°N) is used for calculating the LLJ index and the white contour line is the geopotential height (m). The reference wind vector is 5 m/s. **(b)** Mean vertical profile of the fire tracer (color coding) over 96.25-94.375°W, 18-30.5°N (white box in the left figure) as a function of latitude with wind vectors (black arrows) (reference wind vector: 3 m/s).

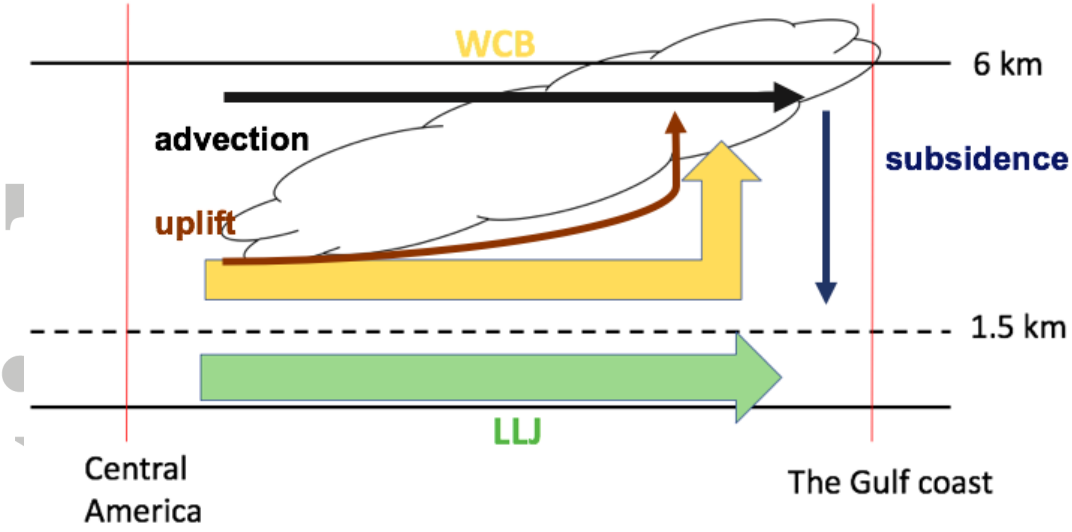

Figure 3. Conceptual model of transport mechanisms from Central America to the US Gulf Coast. The main transport mechanisms include Warm Conveyor Belt (WCB) related with mid-latitude cyclones and Low-Level Jet (LLJ). Other transport mechanisms such as subsidence, uplift, and advection are also included.

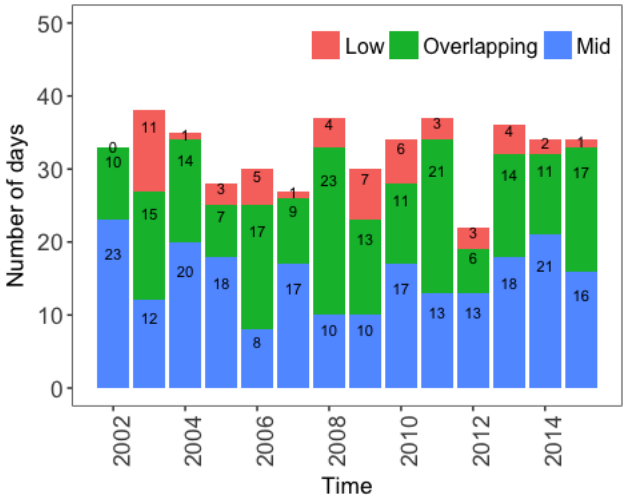

Figure 4. The number of low-altitude events (red; excluding those overlapped with mid-altitude events), mid-altitude events (blue; excluding those overlapped with low-altitude events), and the overlapping events (green) for April and May in each year from 2002-2015.

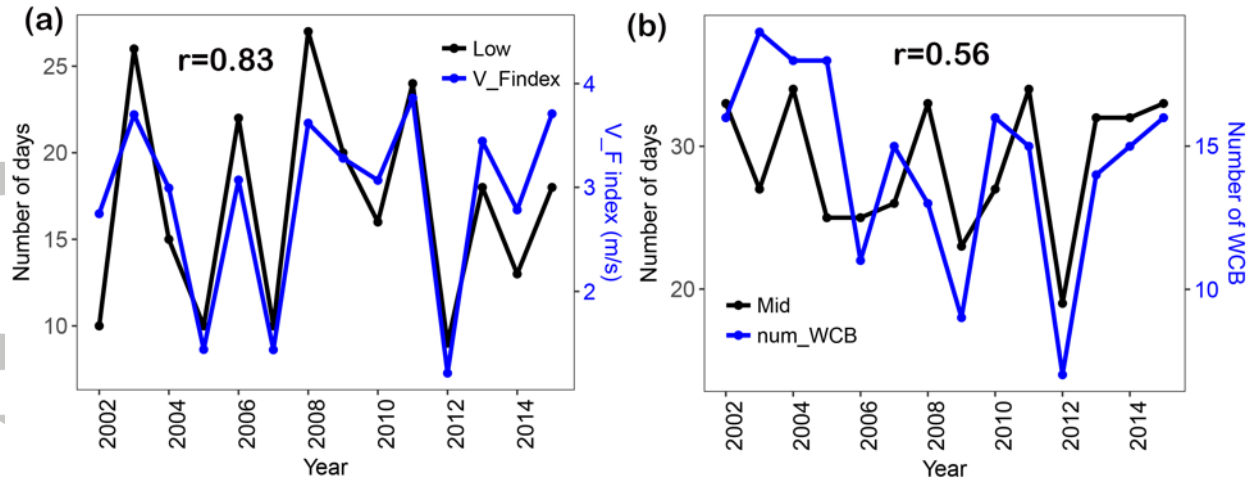

Figure 5. (a) Time series of the number of low-altitude events and V_F index. **(b)** Time series of the number of mid-altitude events and the total number of identified WCB events.

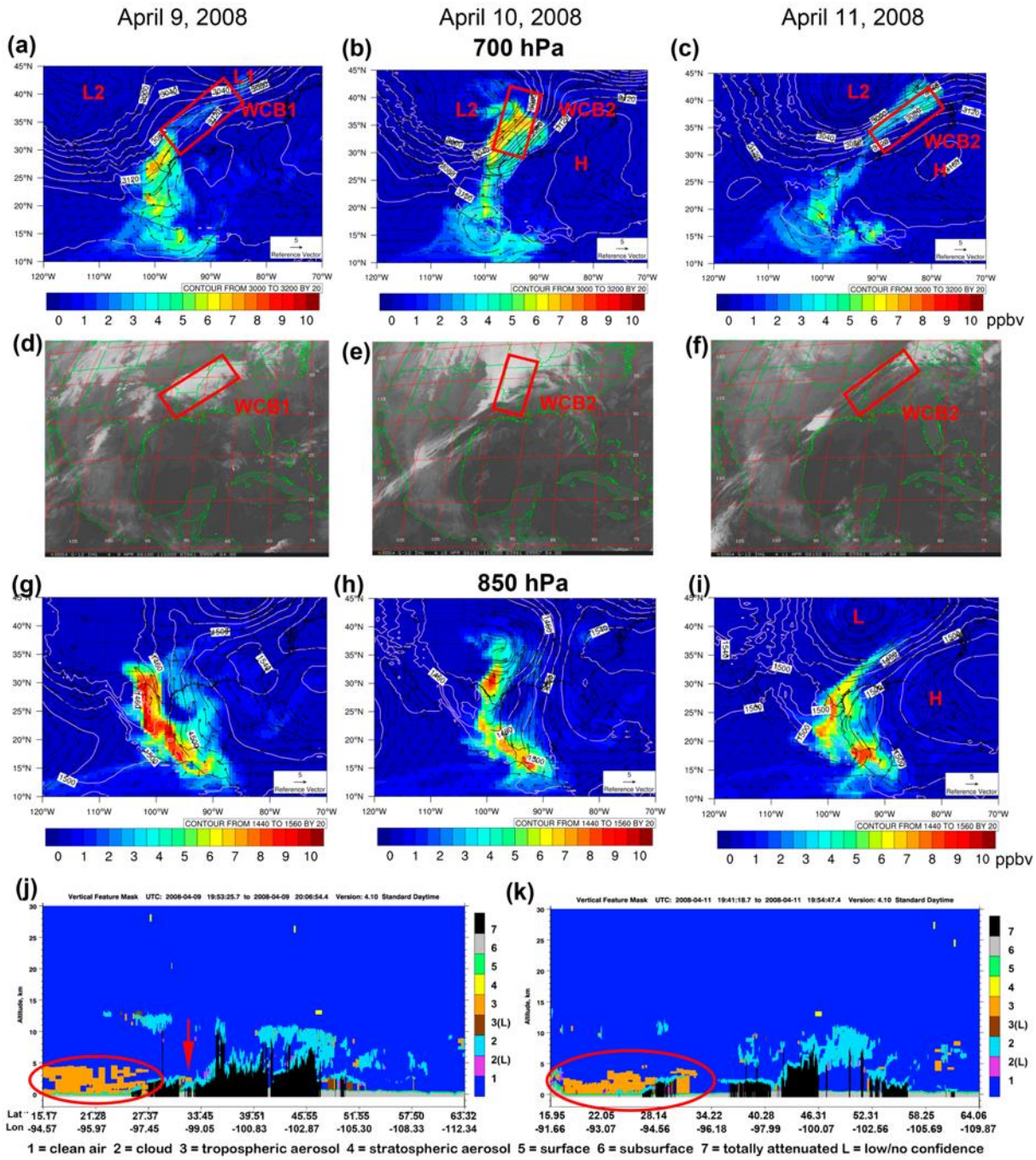

Figure 6. Top row: Simulated fire tracer (filled color contours) overlaid with MERRA2 wind fields (black arrows) and geopotential height (pink contours) at 700 hPa at 6:00 am (local time) on **(a)** April 9, **(b)** April 10, **(c)** April 11, 2008. Second row: GOES Imager observations at 6:00 am (local time) during **(d)** Apr 9, **(e)** 10, and **(f)** 11. Third row: same as the top row, but for 850 hPa. Bottom-row: CALIPSO vertical feature mask on **(j)** Apr 9 at approximately 19:26 UTC (14:26 local time) and **(k)** Apr 11 at approximately 19:14 UTC (14:14 local time).

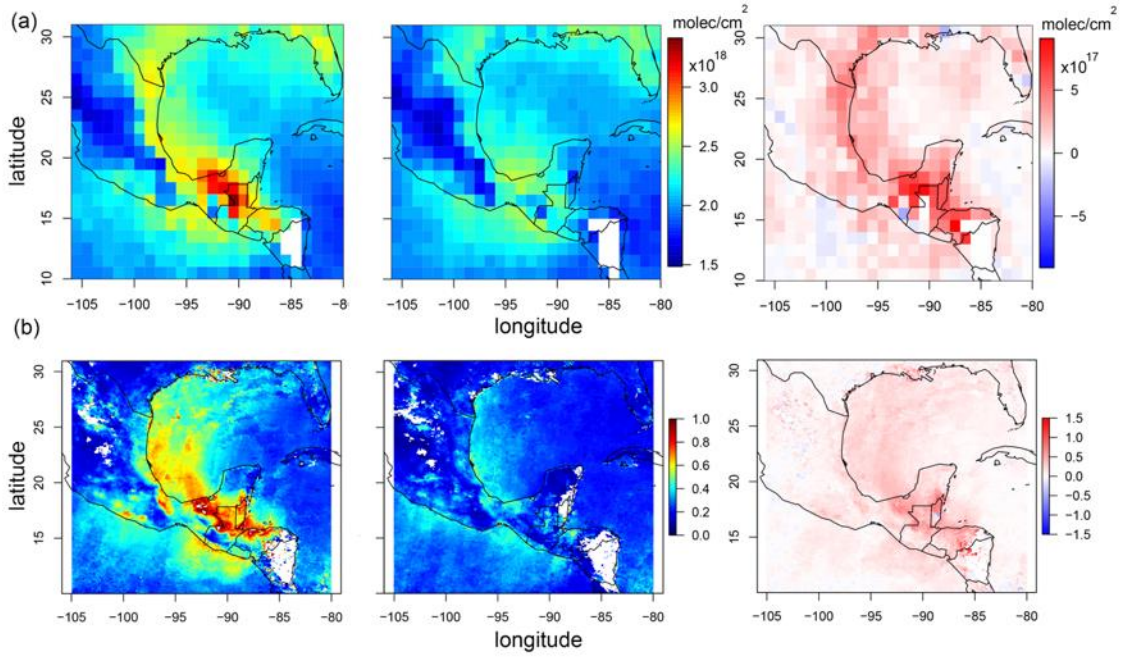

Figure 7. (a) MOPITT CO total column observations for the fire-impact days (left), clean-Gulf days (middle), and the difference between fire-impact days and clean-Gulf days (right). **(b)** MODIS AOD observations from Terra satellite for the fire-impact days (left), clean-Gulf days (middle), and the difference between fire-impact days and clean-Gulf days (right). The sampling period is for April and May 2002 - 2015.

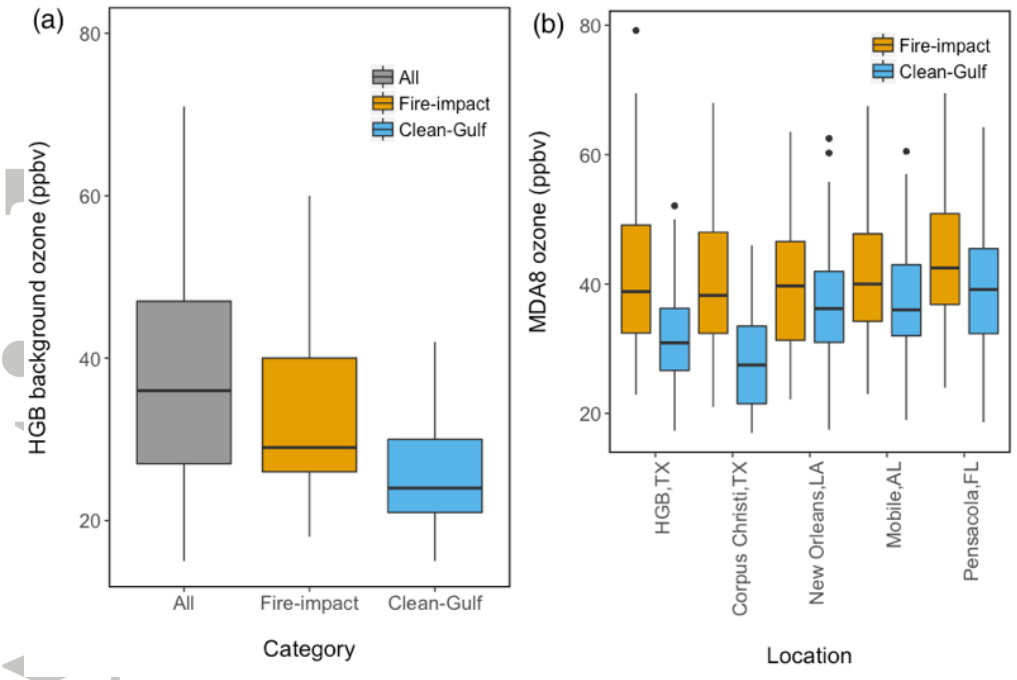

Figure 8. (a) Background ozone distribution of all the days, the fire-impact days and clean-Gulf days over the HGB for the study period. **(b)** MDA8 ozone distribution for the Gulf Coast cities during the fire-impact days and clean-Gulf days. The bottom and the top of each box represent the first (Q1) and the third quartile (Q3), respectively. The horizontal line in each box shows the median, and the two vertical lines outside each box extend to the highest and lowest observations. The outliers are displayed as filled circles, whose values are larger (smaller) than Q3 (Q1) by at least 1.5 times the interquartile range (IQR; Q3-Q1).

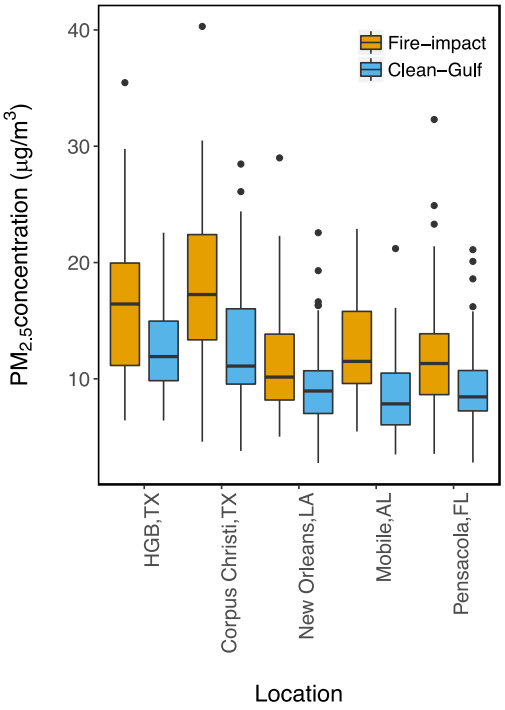

Figure 9. PM2.5 distribution for the Gulf Coast cities during the fire-impact days and clean-Gulf days. The bottom and the top of each box represent the first (Q1) and the third quartile (Q3), respectively. The horizontal line in each box shows the median, and the two vertical lines outside each box extend to the highest and lowest observations. The outliers are displayed as filled circles, whose values are larger (smaller) than Q3 (Q1) by at least 1.5 times the interquartile range (IQR; Q3-Q1).